

AD-A107 040 DAVID W TAYLOR NAVAL SHIP RESEARCH AND DEVELOPMENT CE--ETC F/O 11/6  
DYNAMIC J SUB I-R CURVE TESTING OF HY-130 STEEL.(U)  
OCT 81 J A JOYCE, E J CZYRYCA  
UNCLASSIFIED

DAVID W TAYLOR NAVAL SHIP RESEARCH AND DEVELOPMENT CE--ETC F/G 11/6  
DYNAMIC J SUB I-R CURVE TESTING OF HY-130 STEEL.(U)  
OCT 81 J A JOYCE, E J CZRYCA

UNCLASSIFIED DTNSRDC/SNE-81/57

NP

1000  
2000  
3000  
4000  
5000  
6000  
7000  
8000  
9000  
10000  
11000  
12000  
13000  
14000  
15000  
16000  
17000  
18000  
19000  
20000  
21000  
22000  
23000  
24000  
25000  
26000  
27000  
28000  
29000  
30000  
31000  
32000  
33000  
34000  
35000  
36000  
37000  
38000  
39000  
40000  
41000  
42000  
43000  
44000  
45000  
46000  
47000  
48000  
49000  
50000  
51000  
52000  
53000  
54000  
55000  
56000  
57000  
58000  
59000  
60000  
61000  
62000  
63000  
64000  
65000  
66000  
67000  
68000  
69000  
70000  
71000  
72000  
73000  
74000  
75000  
76000  
77000  
78000  
79000  
80000  
81000  
82000  
83000  
84000  
85000  
86000  
87000  
88000  
89000  
90000  
91000  
92000  
93000  
94000  
95000  
96000  
97000  
98000  
99000  
100000

END  
DATE  
FILMED  
12 84  
RTHC

END  
DATE  
FILMED  
12 84

12

LEVEL II

DTNSRDC/SME 81-57

**DAVID W. TAYLOR NAVAL SHIP  
RESEARCH AND DEVELOPMENT CENTER**

Bethesda, Maryland 20084



AD A107040

DYNAMIC  $J_I$ -R CURVE TESTING OF

HY-130 STEEL

by

J. A. Joyce

Associate Professor, Department of Mechanical Engineering,  
United States Naval Academy  
Annapolis, Maryland

and

E. J. Czyryca

David Taylor Naval Ship Research and Development Center  
Annapolis, Maryland

**DTIC**  
**ELECTE**  
NOV 10 1981

**B**

APPROVED FOR PUBLIC RELEASE; DISTRIBUTION UNLIMITED

SHIP MATERIALS ENGINEERING DEPARTMENT  
RESEARCH AND DEVELOPMENT REPORT

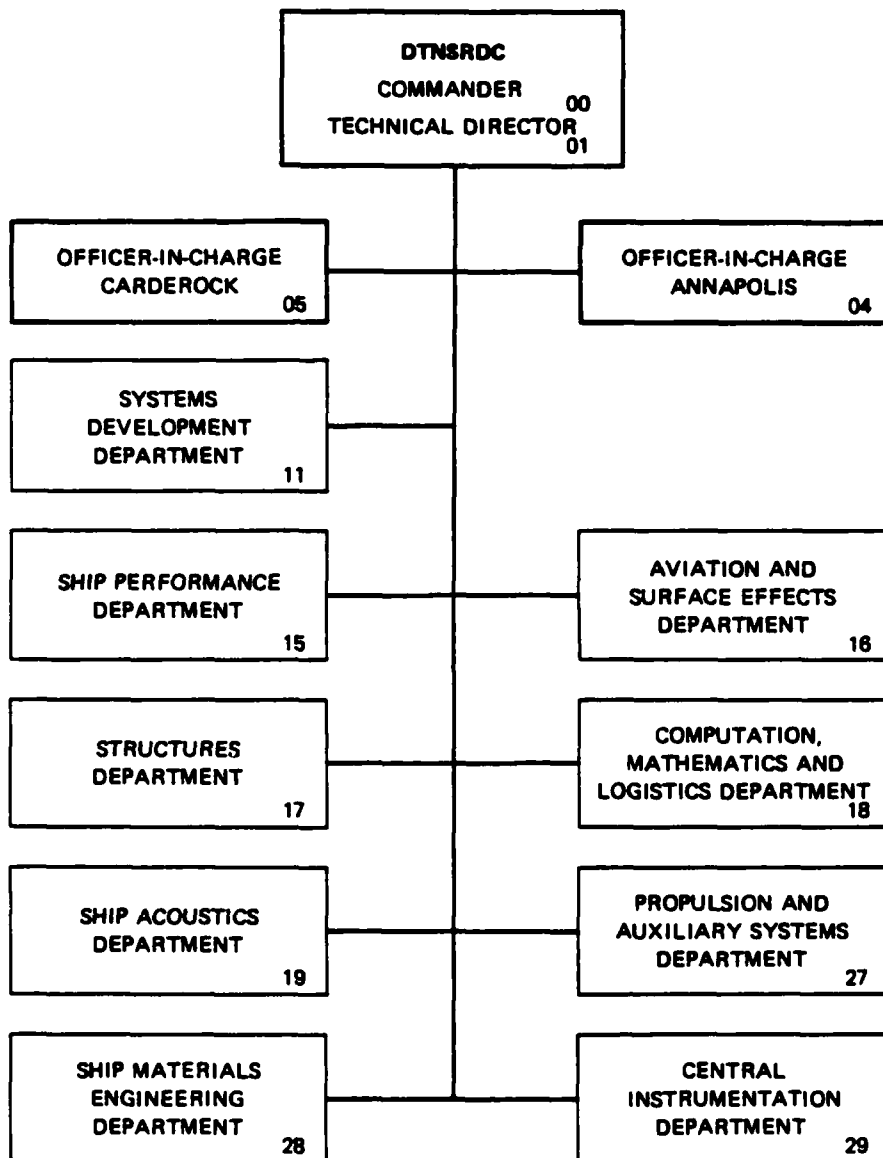
DTIC FILE COPY

October 1981

DTNSRDC SME 81-57

DYNAMIC  $J_I$ -R CURVE TESTING OF HY-130 STEEL

# MAJOR DTNSRDC ORGANIZATIONAL COMPONENTS



14

DTNS

UNCLASSIFIED

SECURITY CLASSIFICATION OF THIS PAGE (When Data Entered)

REPORT DOCUMENTATION PAGE		READ INSTRUCTIONS BEFORE COMPLETING FORM
1. REPORT NUMBER SME-81/57	2. GOVT ACCESSION NO. 46-4267	3. RECIPIENT'S CATALOG NUMBER 40 (and)
4. TITLE (and Subtitle) DYNAMIC CURVE TESTING OF HY-130 STEEL	5. TYPE OF REPORT & REMOD COVERED Research & Development	6. PERFORMING ORG. REPORT NUMBER
7. AUTHOR(s) J. A. Joyce and E. J. Czyryca	8. CONTRACT OR GRANT NUMBER(s) (16) F61342	
9. PERFORMING ORGANIZATION NAME AND ADDRESS Naval Sea Systems Command (SEA 05R15) Washington, DC 20362	10. PROGRAM ELEMENT, PROJECT, TASK AREA & WORK UNIT NUMBERS (17) Program Element 62761N Task Area SF/61-541-592 Work Unit 1-2803-161	
11. CONTROLLING OFFICE NAME AND ADDRESS David Taylor Naval Ship R&D Center Annapolis, Maryland 21402	12. REPORT DATE (11) October 1981	13. NUMBER OF PAGES (12) 35/
14. MONITORING AGENCY NAME & ADDRESS (if different from Controlling Office)	15. SECURITY CLASS. (of this report) UNCLASSIFIED	15a. DECLASSIFICATION/DOWNGRADING SCHEDULE
16. DISTRIBUTION STATEMENT (of this Report) APPROVED FOR PUBLIC RELEASE, DISTRIBUTION UNLIMITED		
17. DISTRIBUTION STATEMENT (of the abstract entered in Block 20, if different from Report)		
18. SUPPLEMENTARY NOTES		
19. KEY WORDS (Continue on reverse side if necessary and identify by block number) Fracture mechanics      Dynamic Fracture J-integral      Key Curve Method HY-130 Steel      Fractography J <sub>I</sub> -R Curves		
20. ABSTRACT (Continue on reverse side if necessary and identify by block number) The J-integral crack growth resistance properties of HY-130 steel were developed under dynamic loading conditions. The objective of this program was to extend the key curve method to evaluate ductile fracture properties of HY-130 steel compact specimens where the loading rate produced a load-line crack-opening displacement rate on the order of 9-inches per second. A key curve for HY-130 plate was developed under dynamic loading conditions using subsized specimens and was applied to tests of ITCT Specimens. Results of ambient temperature tests showed that both J <sub>Ic</sub> and the tearing modulus of this steel were substantially elevated under dynamic loading. The fracture process of specimens tested under dynamic and static loading conditions was found to be similar and completely ductile.		

DD FORM 1 JAN 73 1473

EDITION OF 1 NOV 65 IS OBSOLETE  
S/N 0102-LF-014-6601

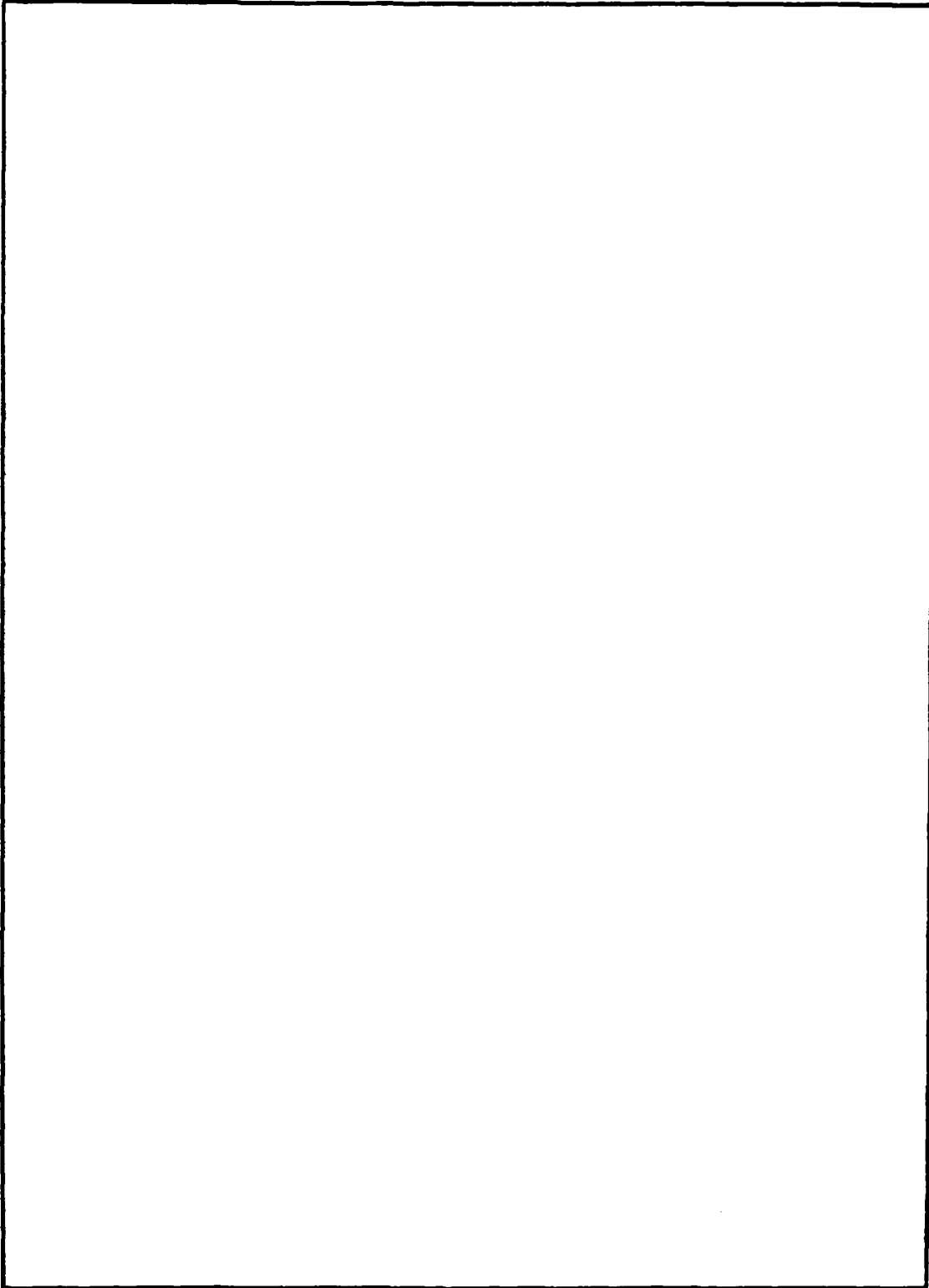
UNCLASSIFIED

SECURITY CLASSIFICATION OF THIS PAGE (When Data Entered)

i/ii

UNCLASSIFIED

SECURITY CLASSIFICATION OF THIS PAGE (When Data Entered)



UNCLASSIFIED

SECURITY CLASSIFICATION OF THIS PAGE (When Data Entered)

## TABLE OF CONTENTS

	Page
LIST OF FIGURES .....	iii
LIST OF TABLES .....	iv
NOMENCLATURE .....	v
LIST OF ABBREVIATIONS .....	vi
ABSTRACT .....	1
ADMINISTRATIVE INFORMATION .....	1
INTRODUCTION .....	1
BACKGROUND .....	1
SCOPE .....	2
KEY CURVE ANALYSIS .....	2
KEY CURVE FUNCTION FILE .....	3
$J_I$ - $R$ CURVE ANALYSIS .....	4
COMPUTATIONAL PROCEDURES .....	5
CRACK GROWTH CORRECTIONS .....	6
EXPERIMENTAL PROCEDURE .....	7
MATERIAL .....	8
TEST METHODS .....	8
RESULTS AND DISCUSSION .....	9
CONCLUSIONS .....	12
ACKNOWLEDGMENT .....	13
REFERENCES .....	25

## LIST OF FIGURES

1 - Experimental Key Curve Function for HY-130 Steel for Static Loading Rate .....	14
2 - HY-130 $J_I$ - $R$ Curves Developed by Key Curve Analysis and Unloading Compliance Under Static Loading Conditions .....	15
3 - Modified 1-Inch-Thick (25.4-mm) Compact Test Specimen for $J$ -Integral Testing .....	16
4 - Modified 1/2-Inch-Thick (12.7-mm) Compact Test Specimen for $J$ -Integral Testing .....	17
5 - Schematic of Compact Specimen Dynamic Test Arrangement .....	18
6 - Experimental Key Curve Function for HY-130 Steel Obtained Under Dynamic Loading .....	19

	Page
7 - Load-Displacement Curves for 1-Inch-Thick (25.4-mm) Compact Test Specimens of HY-130 Steel Tested Under Dynamic Loading Conditions .....	19
8 - J-Integral R-Curve for 1-Inch-Thick (25.4-mm) Compact Test Specimens of HY-130 Steel Tested Under Dynamic Loading Conditions .....	20
9 - J-Integral R-Curves for 1-Inch-Thick (25.4-mm) Compact Test Specimens of HY-130 Steel Tested Under Static and Dynamic Loading Conditions .....	20
10 - Load-Line Crack-Opening Displacement Rate Versus Crack-Opening Displacement for a Typical 1-Inch-Thick (25.4-mm) Compact Test Specimen of HY-130 Steel Tested Under Dynamic Loading Conditions .....	21
11 - $dJ/dt$ Versus Crack-Opening Displacement for a Typical 1-Inch-Thick (25.4-mm) Compact Test Specimen of HY-130 Steel Tested Under Dynamic Loading Conditions .....	22
12 - $dJ/dt$ Versus Elapsed Time for a Typical 1-Inch-Thick (25.4-mm) Compact Test Specimen of HY-130 Steel Tested Under Dynamic Loading Conditions .....	22
13 - Crack Extension Rate (Crack Velocity) Versus $J_I$ for a Typical 1-Inch-Thick (25.4-mm) Compact Test Specimen of HY-130 Steel Under Dynamic Loading Conditions .....	23
14 - Scanning Electron Fractographs of HY-130 Steel Ductile Fracture Crack Extension Under Static and Dynamic Loading (400X) .....	24

#### LIST OF TABLES

1 - Chemical Composition of HY-130 Steel .....	8
2 - Tensile Mechanical Properties of HY-130 Steel .....	8
3 - Summary of $J_I$ -R Curve Parameters from Dynamic Fracture Tests .....	10
4 - Comparison of HY-130 $J_I$ -R Curve Parameters from Static and Dynamic Fracture Tests .....	11

# NOMENCLATURE

$P$	Load
$W$	Specimen width
$a$	Crack length
$b$	Uncracked ligament
$B$	Specimen thickness, nominal
$B_n$	Net specimen thickness
$\sigma_o$	Flow stress
$H$	Specimen height
$P_L$	Limit load
$\Delta$	Crack-opening displacement at the load line
$\eta$	Crack growth correction parameter
$\gamma$	Crack growth correction parameter
$A$	Area under load versus displacement curve
$T$	Tearing modulus
$E$	Modulus of elasticity
$P_{max}$	Maximum load

Accession For	
ADVISORY	<input checked="" type="checkbox"/>
LIBRARY	<input type="checkbox"/>
EXHIBIT	<input type="checkbox"/>
Classification	
Distribution/	
Availability Codes	
Avail and/or	Special
Dist	
<b>A</b>	

## LIST OF ABBREVIATIONS

ASTM	American Society for Testing and Materials
°C	Degrees Celsius
COD	Crack-opening displacement
CT	Compact tension
CVN	Charpy V-notch
dia	Diameter
in-lb/in <sup>2</sup>	Inch-pound per square inch
ips	Inch per second
$J_I$ -R Curve	Crack extension resistance curve in terms of $J_I$
ksi	Thousand pounds per square inch
ksi-in/sec	Thousand pound-inch per square inch per second
max	Maximum
MPa	Megapascal
μm	Micrometer
μsec	Microsecond
mm	Millimeter
psi	Pounds per square inch
R	Radius
1TCT	One-inch-thick (25.4-mm) compact tension specimen
½TCT	One-half-inch-thick (12.7-mm) compact tension specimen
T-L	Transverse-longitudinal crack plane orientation
$\sigma_{UTS}$	Ultimate tensile strength
$\sigma_{YS}$	Yield strength (0.2% offset)

## ABSTRACT

The J-integral crack growth resistance properties of HY-130 steel were developed under dynamic loading conditions. The objective of this program was to extend the key curve method to evaluate ductile fracture properties of HY-130 steel compact specimens where the loading rate produced a load-line crack-opening displacement rate on the order of 9-inches per second. A key curve for HY-130 plate was developed under dynamic loading conditions using subsized compact specimens and was applied to tests of 1TCT specimens. Results of ambient temperature tests showed that both  $J_{Ic}$  and the tearing modulus of this steel were substantially elevated under dynamic loading. The fracture process of specimens tested under dynamic and static loading conditions was found to be similar and completely ductile.

## ADMINISTRATIVE INFORMATION

This report was prepared as part of the Surface Ship and Craft Materials Technology Block Program under the sponsorship of Dr. H.H. Vanderveldt, Naval Sea Systems Command (SEA 05R15). The effort was supervised by Mr. John P. Gudas at this Center under Program Element 62761N, Task Area SF-61-541-592, Work Unit 1-2803-161. This report satisfies Milestone RQ 1.6/1 from the July 1980 Surface Ship and Craft Block Plan.

## INTRODUCTION

### BACKGROUND

During the past several years, efforts in the area of quantitative elastic-plastic fracture mechanics have centered on the J-integral methods introduced by Rice,<sup>1\*</sup> and the  $J_{Ic}$  parameter and  $J_I-R$  curve introduced by Landes and Begley<sup>2</sup> and Paris.<sup>3</sup> A proposed standard method for determination of the  $J_{Ic}$  parameter is nearing adoption by the American Society for Testing and Materials<sup>4</sup> which will enhance utilization of the concepts in advanced analyses. Many questions remain, however, concerning the meaning and application of the  $J_I-R$  curve beyond the point of crack initiation. Recent work by Paris, et al,<sup>5</sup> and by Joyce and Vassilaros<sup>6</sup> has shown that the tearing modulus, which is related to the slope of the  $J_I-R$  curve, can be used to predict the onset of ductile tearing instability in laboratory specimens tested in compliant test machines. Experimental studies to evaluate the specimen geometry dependence of the  $J_I-R$  curve have been completed by Gudas.

\*A complete list of references appears on page 25.

et al,<sup>7</sup> and Vassilaros, et al,<sup>8</sup> and have shown the tearing modulus to be nearly independent of specimen geometry in side-grooved compact specimens of HY-130 and A533B steels. When side grooves are not present, however, and crack tunneling occurs, the tearing modulus can be increased by 20% to 50% in comparison with side-grooved specimens of the identical material.

Equally as important as the effect of geometry on  $J_{Ic}$  and the  $J_I-R$  curve is the effect of loading rate. The basic methods used to date to evaluate the  $J_I-R$  curve have been the multispecimen method of Landes and Begley<sup>2</sup> and the unloading compliance method of Clarke, et al.<sup>9</sup> Neither of these methods is readily adaptable to dynamic testing. Studies have been conducted at rapid loading rates,<sup>10-12</sup> but primarily to define  $J_{Ic}$  and not to determine the shape of the  $J_I-R$  curve.

A method of  $J_I-R$  curve determination which is readily adaptable to high rate testing is the "key curve" function method or calibration function method introduced by Ernst, et al,<sup>13</sup> and applied by Joyce, et al,<sup>14</sup> to static tests on HY-130. The key curve analysis technique is used to obtain the  $J_I-R$  curve of an elastic-plastic material directly from the load versus crack-opening displacement (COD)\* record without use of ancillary methods of crack length determination. The method does require a key curve function for the particular specimen geometry, material, and test rate which is empirically determined.

## SCOPE

The objective of this task was to utilize the key curve method to determine  $J_I-R$  curves for HY-130 compact specimens at a loading rate which produced a crack opening rate of 9 ips at the specimen load line and to evaluate the effect of this rate increase on the  $J_{Ic}$  parameter and on the shape of the  $J_I-R$  curve for an HY-130 steel. To accomplish this, compact specimens of an HY-130 plate, for which extensive static  $J_I-R$  curve data were available, were tested in a fast-acting servo hydraulic test machine. Load-displacement data were taken by a high precision, digital oscilloscope interfaced with a minicomputer. These data were then analyzed using the method of Joyce, et al,<sup>14</sup> to produce dynamic  $J_I-R$  curves for comparison with the static results.

Prior to a description of the experimental work, the principles of the key curve method, computational procedures, and its application in determining the  $J_I-R$  curve in static tests are described.

## KEY CURVE ANALYSIS

A key curve function as introduced by Ernst, et al,<sup>13</sup> represents a load-displacement relationship for a particular specimen type in the form:

\*Definitions of abbreviations used are given on page vi.

$$\frac{PW}{Bb^2} = F_1 \left( \frac{\Delta}{W}, \frac{a}{W}, \frac{H}{W}, \frac{B}{W}, \text{material properties} \right) \quad (1)$$

where:

$P$  = Applied load

$W$  = Specimen width

$\Delta$  = Total load-line COD

$B$  = Specimen thickness

$H$  = Specimen height

$b = W - a$  = Specimen uncracked ligament

$a$  = Crack length.

The fact that such a relationship does exist for simple geometries in which the plasticity is confined to the uncracked ligament region was shown by Rice.<sup>15</sup> If an investigation is conducted with specimens of the same material machined to be geometrically similar, only three of the variables are present in the function:

$$\frac{PW}{Bb^2} = F_1 \left( \frac{\Delta}{W}, \frac{a}{W} \right). \quad (2)$$

The premise for the key curve analysis is that load-displacement records for geometrically similar specimens of the same material with identical crack ligament ( $a/W$ ) ratios will trace identical lines when plotting normalized load ( $PW/Bb^2$ ) as a function of  $\Delta/W$ , up to the point of crack initiation. A specimen in which crack extension occurred would then fall below an uncracked specimen (in normalized load,  $PW/Bb^2$ ) at a given value of  $\Delta/W$ .

#### KEY CURVE FUNCTION FILE

A key curve function may be obtained experimentally by loading and recording crack-opening displacement for a series of identical CT specimens with a range of crack lengths. The load-displacement records are useful only up to the  $\Delta/W$  value for crack initiation. These load-displacement records are then smoothed and assembled in a key curve file as an approximate representation of the function of Equation (2).

A key curve obtained experimentally in static tests of HY-130 and reported by Joyce, et al.,<sup>14</sup> is shown in Figure 1. This function can be taken to represent the load-displacement behavior of all geometrically similar compact specimens of this material of any crack length ratio. If no crack extension were to occur, a load-displacement record for a particular specimen would exist at the cross section given by the specimen's original  $a/W$  ratio. If crack extension occurred, the true load-displacement record would shift across the key curve surface in a more complex manner.

### $J_I$ - $R$ CURVE ANALYSIS

Once the experimental key curve file is established,  $J_I$ - $R$  curves may be obtained from single-specimen tests by the following analysis of Ernst, et al.<sup>13</sup> Assuming that deformation plasticity theory is applicable, the formula for the path independent J-integral<sup>1</sup> is given by:

$$J = \frac{-1}{W} \int_0^{\Delta} \left( \frac{\partial P}{\partial (a/W)_{\Delta}} \right) d\Delta. \quad (3)$$

Substituting for  $P$  from Equation (2) into Equation (3) gives  $J$  as:

$$J = - \int_0^{\Delta} \left( \frac{b^2}{W^2} \frac{\partial F_1}{\partial (a/W)} - \frac{2b}{W} F_1 \right) d\Delta. \quad (4)$$

The differential of  $J$  can be written as

$$dJ = \frac{\partial J}{\partial \Delta} d\Delta + \frac{\partial J}{\partial a} da. \quad (5)$$

Now, evaluating from Equation (4) the terms of Equation (5), and substituting in Equation (5) gives:

$$\begin{aligned} dJ = & \left[ \frac{2b}{W} F_1 - \frac{b^2}{W^2} \frac{\partial F_1}{\partial (a/W)} \right] d\Delta \\ & + \left[ \int_0^{\Delta} - \frac{2}{W} F_1 d\Delta + \int_0^{\Delta} \frac{4b}{W^2} \frac{\partial F_1}{\partial (a/W)} d\Delta \right. \\ & \left. + \int_0^{\Delta} \frac{b^2}{W^3} \frac{\partial^2 F_1}{\partial (a/W)^2} d\Delta \right] da. \end{aligned} \quad (6)$$

This differential expression can now be reintegrated along any convenient path in the  $a/W - \Delta/W$  space to obtain  $J$ , at least if the partial derivatives  $\partial F_1 / \partial (a/W)$  and  $\partial^2 F_1 / \partial (a/W)^2$ , and the differential crack extension,  $da$ , are somehow available. To obtain an expression for differential crack extension, Ernst, et al.<sup>13</sup> take the differential of Equation (1) with  $\Delta/W$  and  $a/W$  as variables to give:

$$dP = \frac{\partial P}{\partial \Delta} d\Delta + \frac{\partial P}{\partial a} da. \quad (7)$$

Evaluating the coefficients in terms of  $F_1$  gives

$$dP = \frac{b^2}{W^2} \frac{\partial F_1}{\partial (\Delta/W)} d\Delta + \left[ \frac{b^2}{W^2} \frac{\partial F_1}{\partial (a/W)} - \frac{2b}{W} F_1 \right] da. \quad (8)$$

Solving for  $da$  gives

$$da = \frac{\frac{b^2}{W^2} \frac{\partial F_1}{\partial (\Delta/W)} d\Delta - dP}{\frac{2b}{W} F_1 - \frac{b^2}{W^2} \frac{\partial F_1}{\partial (a/W)}}. \quad (9)$$

$J_I$ - $R$  curves may be obtained from a single specimen test load-displacement record and the key curve file assembled from geometrically similar specimens of the same material by numerical methods. Incremental computation of Equations (6) and (9) for  $J_I$  (corrected for crack extension<sup>14</sup>) and crack extension, respectively, is required. Terms involving  $F_1$  or  $dP$  are evaluated from the single-specimen load-displacement record, while terms involving derivatives of  $F_1$  are obtained from the key curve file.

## COMPUTATIONAL PROCEDURES

To obtain  $J_I$ - $R$  curves directly from the load-displacement curves, discrete versions of Equations (6) and (9) were written,

$$\begin{aligned} \delta J_n = & \left[ \frac{2b}{W} F_{1n} - \frac{b^2}{W^2} \left( \frac{\partial F_1}{\partial (a/W)} \right)_n^* \right] \delta \Delta_n \\ & + \left[ - \frac{2}{W} \sum_{i=1}^n F_{1i} \delta \Delta_i + \frac{4b}{W^2} \sum_{i=1}^n \left( \frac{\partial F_1}{\partial (a/W)} \right)_i^* \delta \Delta_i \right. \\ & \left. + \frac{b}{W^3} \sum_{i=1}^n \left( \frac{\partial^2 F_1}{\partial (a/W)^2} \right)_i^* \delta \Delta_i \right] \delta a_n \end{aligned} \quad (10)$$

and

$$\delta a_n = \frac{\frac{b^2}{W^2} \left( \frac{\partial F_1}{\partial (\Delta/W)} \right)_n^* \delta \Delta_n - \delta P_n}{\frac{2b}{W} F_{1n} - \frac{b^2}{W^2} \left( \frac{\partial F_1}{\partial (a/W)} \right)_n^*} \quad (11)$$

At each point,  $m$ , on the load-displacement record of a specimen, the total  $J$  and  $\Delta a$  are:

$$J = \sum_{n=1}^m \delta J_n \quad (12)$$

$$\Delta a = \sum_{n=1}^m \delta a_n \quad (13)$$

In Equations (10) and (11) the terms without asterisks are evaluated from the specimen load-displacement curve. The terms with asterisks were evaluated from the  $F_1$  key curve file. A computer program was written which evaluated Equations (10) through (13), generating for each point on the digital load-displacement record of each specimen a pair;  $\Delta a$ ,  $J$ ; on a  $J_I$ - $R$  Curve for the specimen. Each point,  $n$ , of the load-displacement record gives  $F_{1n}$  and  $\delta P_n$  directly. The measured crack length, obtained by a heat tint, 9-point average measurement after testing, and the  $\Delta/W$  at each point of the load-displacement record locates a position on the  $F_1$  key curve function for the material (see Figure 1). Numerical differentiation techniques are used about this point to determine

$$\left( \frac{\partial F_1}{\partial (a/W)} \right)_n^* \text{ and } \left( \frac{\partial F_1}{\partial (\Delta/W)} \right)_n^* \quad (14)$$

These values give  $\delta a_n$  from Equation (11) and subsequently  $\delta J_n$  from Equation (10). Summations of these quantities using Equations (12) and (13) give running totals of  $J$  and  $\Delta a$ . Performing these computations for complete load-displacement records for individual specimens results in the individual  $J_I$ - $R$  curves for those specimens.

## CRACK GROWTH CORRECTIONS

In the previous work by Joyce, et al.<sup>14</sup> Equations (6) and (9) were used along with the key curve file of Figure 1 to obtain  $J_I$ - $R$  curves for statically loaded compact specimens of HY-130 steel. One of the objectives of this early key curve work was to assess the magnitude of the effect on  $J$  of crack extension, since it was recognized at that time that the key curve analysis did include crack growth corrections. It was determined

that crack growth does have a large effect on  $J$ , and accurate crack growth corrections are essential for the development of meaningful  $J_I$ - $R$  curves. The recent work of Ernst, et al,<sup>16</sup> has provided a methodology for correcting standard unloading compliance results. The Ernst equation for corrected  $J$  is:

$$J_{(i+1)} = [J_i + (\eta/b)_i \frac{A_{i,i+1}}{B_n}] [1 - (\gamma/b)_i (a_{i+1} - a_i)], \quad (15)$$

where:

$$\eta = 2 + (0.522) b/W$$

$$\gamma = 1 + 0.76 b/W$$

$B_n$  = Net specimen thickness at the side-groove root

$A_{i,i+1}$  = Area under load versus load point displacement record between lines of constant displacement at points  $i$  and  $i + 1$ .

Application of Equation (15) to results previously reported by Gudas, et al,<sup>7</sup> showed that this expression yields  $J_I$ - $R$  curves which are in close agreement with key curve results.

The static  $J_I$ - $R$  curves for HY-130 developed by key curve<sup>14</sup> and unloading compliance tests<sup>7</sup> are compared in Figure 2. In Figure 2, the results for the unloading compliance test are shown as calculated using the Merkle-Corten<sup>17</sup> analysis and using the Ernst<sup>16</sup> analysis (i.e., Equation (15)). Similar results<sup>14</sup> demonstrated the need for crack growth corrections to the J-integral calculation and led to the development of Equation (15).

The agreement between the test methods in developing  $J_I$ - $R$  curves for HY-130, as shown in Figure 2, demonstrates the equivalency of the methods. Recent key curve test results developed for ASTM A533B steel<sup>18</sup> also support the use of the key curve method to determine  $J_I$ - $R$  curves directly from load-displacement records.

## EXPERIMENTAL PROCEDURE

The experimental phase of this task involved testing a series of HY-130 compact specimens at a load-line  $COD$  rate of 9 *ips*. Load-displacement curves from these specimens were then analyzed by the key curve analysis technique to develop  $J_I$ - $R$  curves. A key curve function was developed experimentally from high-speed tests on a series of half-scale compact specimens of the same material containing a range of crack lengths.

## MATERIAL

One-inch-thick (25.4-mm) HY-130 plate was used for all tests. The chemical composition of the plate is described in Table 1 and the mechanical properties are presented in Table 2. This was the same plate used in the static key curve analysis<sup>13</sup> and for which  $J$ - $R$  curves were determined by the unloading compliance method.<sup>6</sup>

TABLE 1 — CHEMICAL COMPOSITION OF HY-130 STEEL

Center Code	Chemical Composition (Wt %)												
	C	Mn	P	Si	Ni	Cr	Mo	V	S	Cu	Al	Co	Ti
FKS	0.11	0.76	0.005	0.03	5.00	0.42	0.53	0.043	0.004	0.022	0.021	0.02	0.008

TABLE 2 — TENSILE MECHANICAL PROPERTIES OF HY-130 STEEL

Center Code	$\sigma_{YS}$ Yield Strength 0.2% Offset (ksi (MPa))	$\sigma_{UTS}$ Ultimate Tensile Strength (ksi (MPa))	Elongation in 2-In. (%)	Reduction of Area (%)
FKS	136 (937)	142 (978)	21	55

## TEST METHODS

The key curve method requires two sizes of geometrically similar specimens and for this task 1TCT (nominally 1 in. (25.4mm) thick) and 1/2TCT (nominally 1/2 in. (12.7mm) thick) specimens were used. 1TCT and 1/2TCT specimens were machined as shown in Figures 3 and 4, respectively. The 1/2TCT specimen is one-half the scale of the 1TCT specimens except that integral knife edges at the load-line were used on the smaller specimens to accommodate a clip-gage extensometer instead of the screw-fastened razor blades used on the larger specimens. The crack-starter notches were placed in the  $T$ - $L$  orientation. All tests were conducted at ambient temperature in a high-speed servo hydraulic test machine capable of ram velocities of 9 ips.

The specimens were fatigue precracked according to the ASTM proposed standard method for  $J_{IC}$  testing with

$$P_{max} < \frac{1}{3} P_L \quad (16)$$

where  $P_L$  is the specimen limit load given for compact specimens<sup>4</sup> as:

$$P_L = \frac{Bb^2 \sigma_o}{(2W + a)} \quad (17)$$

where:

$$\sigma_o = \frac{\sigma_{YS} + \sigma_{UTS}}{2} \text{ (Table 2) = flow stress.}$$

Precrack lengths for  $1/2TCT$  specimens were varied from  $a/W = 0.51$  to  $a/W = 0.88$ ; those for the  $1TCT$  specimens varied from  $a/W = 0.65$  to  $a/W = 0.80$ . After precracking, face grooves were machined along the crack line to a total section reduction of 20% with a standard Charpy V-notch (CVN) cutter (45° included angle, 0.010-in. (0.254-mm) root radius).

The specimens were then loaded at the maximum extension rate in the test machine using a 5000-lb load cell. Load versus load-line displacement records were obtained using a high-speed digital oscilloscope interfaced with a minicomputer. A schematic of the test apparatus and data acquisition system is shown in Figure 5. Identical tests were then performed on a series of  $1TCT$  specimens with the same apparatus except that a 20,000-lb load cell was used. All load versus load-line displacement records were stored on magnetic tape for subsequent key curve analysis. All tests were conducted at ambient laboratory temperature.

After the tests had been completed, the specimens were heat-tinted at 370°C (700°F) for 30 minutes to mark the final crack extension. The specimens were then fractured at liquid nitrogen temperature to complete separation. The fatigue precrack length and final crack extension were measured at nine equally spaced points across the crack surface excluding the edges.

## RESULTS AND DISCUSSION

The key curve function for HY-130 in this study was obtained from the rapid load versus COD records of the  $1/2TCT$  specimens with crack length ratios ranging from  $a/W = 0.51$  to  $a/W = 0.88$ . The load-displacement records up to the  $\Delta/W$  value for crack initiation (at maximum load for these specimens) were smoothed and assembled in a key curve file. The key curve file that resulted from the dynamic loading is shown in Figure 6. This file represented approximately 4000 triples of  $PW/Bb^2$ ,  $a/W$ , and  $\Delta/W$  assembled in a single file so that the quantities needed to evaluate Equations (6) and (9) could be obtained using methods of numerical analysis. This key curve file is different than that shown for static loading in Figure 1 in that it is elevated in load ( $PW/Bb^2$  scale) due to the high loading rate. Representative load-displacement curves for the  $1TCT$  specimens are shown in Figure 7.

The  $J_I$ - $R$  curves obtained from 1TCT specimens of varying crack lengths are shown in Figure 8. This figure also includes the measured final crack extension for three of the specimens. The measured final crack extension for Specimen FKS S20 was not included because its load-displacement curve extended beyond the range of  $\Delta/W$  to which the key curve file of Figure 6 is applicable. The predicted crack extension agreed very well with that measured for two specimens, with the third showing a 20% shortfall of the estimated value. Taken together, the results shown in Figure 8 define the  $J_I$ - $R$  curve for the test material at the dynamic loading rate. Figure 9 shows a comparison of the dynamic  $J_I$ - $R$  curves and the previously reported results of Gudas, et al.<sup>5</sup> for the same HY-130 plate. The static results are corrected for crack growth according to Equation (15). Table 3 summarizes the  $J_I$ - $R$  curve parameters from the dynamic tests including values of the Paris material tearing modulus<sup>5</sup> defined as:

$$T_{MAT} = \frac{dJ}{da} \cdot \frac{E}{\sigma_o 2}, \quad (18)$$

TABLE 3 — SUMMARY OF  $J_I$ - $R$  CURVE PARAMETERS FROM DYNAMIC FRACTURE TESTS

Specimen No.	Cracked Ligament Ratio $a/W$	$J_{Ic}$ (in-lb/in <sup>2</sup> )	Tearing Modulus $T_{MAT}$
FKS S20	0.65	1140	40.0
FKS S25	0.66	1321	28.1
FKS S1	0.76	1533	27.9
FKS S16	0.80	1248	26.7
Notes: 1TCT Specimens - 20% side groove. Load-line COD rate - 9 ips.			

where  $E$  = Modulus of Elasticity =  $29 \times 10^6$  psi.

For 1TCT specimens,  $J_{Ic}$  values were computed from the intersection of the crack-opening stretch line ( $J = 2\sigma_y \cdot \Delta a$ ) with the least squares fit of data points which fell at least 0.006 in. (0.15mm) beyond the blunting line and did not exceed 0.06 in. (1.5 mm) in crack growth from that point. Tearing moduli were calculated using the same range of crack extension. The  $J_I$ - $R$  curve parameters for HY-130 from static<sup>7,19</sup> and dynamic tests are compared in Table 4.  $J_{Ic}$  values are calculated here according to the method of Clarke, et al.<sup>4</sup> to be incorporated in the proposed ASTM Standard Method.

TABLE 4 — COMPARISON OF HY-130  $J_I$ - $R$  CURVE PARAMETERS FROM  
STATIC AND DYNAMIC FRACTURE TESTS

	Load-Line COD Rate (ips)	Side Groove (%)	Cracked Ligament Ratio $a/W$	Average $J_{Ic}$ (in-lb/in <sup>2</sup> )	Average Tearing Modulus $T_{MAT}$
Reference 19	$1.6 \times 10^{-4}$	0	0.55	825	19
			0.70	902	19
			0.80	819	28
		12.5	0.55	824	12
			0.70	847	12
			0.80	820	11
		25	0.70	771	12
			0.80	845	14
Present Investigation	9	20	0.65	1230	34
			0.75	1533	28
			0.80	1248	27

The results displayed in Figure 9 and in Table 4 show that the  $J_I$ - $R$  curve parameters for the dynamic tests are elevated by 50% to 100% above those of the static tests. Also note that the tearing modulus values are increased by a factor of about two over those of the side-grooved specimens tested at a slow rate. Previous work by Gudas, et al,<sup>7, 19</sup> has shown that  $J_{Ic}$  and tearing modulus for HY-130, ASTM A533B, ASTM A516 Grade 70, and HY-80 were not a function of side-groove depth beyond an amount sufficient to produce straight, planar crack extension and conservative  $J_I$ - $R$  curves. The difference in the static and dynamic measurement of the parameters  $J_{Ic}$  and tearing modulus shown in Table 4 is a material rate effect and not due to the minor difference in side grooves. Because of the compliance of the test machine and specimen gripping fixtures, the COD rate was not constant during the test. Figure 10 is a plot of typical COD rate obtained by taking the slope of the best-fit straight line fit to 15 COD values over 300- $\mu$ sec intervals over the course of the test. During the rising load portion of the test, the crack-opening displacement was approximately 3 ips. During the falling load portion, the displacement rate was much less stable but averaged 9 ips. Figure 11 shows how the time derivative of  $J$ ,  $dJ/dt$ , varied as a function of crack-opening displacement in a typical test. The maximum value of  $dJ/dt$  occurred at about the  $J_{Ic}$  point with a crack-opening displacement of 0.050 in. (1.27 mm) and then  $dJ/dt$  fell as crack extension took place. Figure 12 shows the rate of applied  $J$  versus time for the same test, and that the maximum  $dJ/dt$  value occurred in about 0.015 sec with this loading apparatus. The crack extension portion of the test had a duration of 0.007 sec during which 0.2 in. (5.08 mm) of crack extension occurred.

An estimate of the crack growth rate was obtained by an iterated numerical differentiation technique using the crack extension values over 400- $\mu$ sec intervals during the course of the test. Results for the preceding example are shown in Figure 13. Crack velocities appear to vary widely but are on the order of 5 to 50 *ips* for these tests. The maximum crack growth rate occurred during the initial region of load drop just beyond the maximum load point. The crack growth rate then decreased with crack extension corresponding to the decrease noted previously in  $dJ/dt$ .

The macroscopic fracture path of the dynamically loaded specimens appeared very similar to that of the static test specimens. Specifically, the degree of crack tunneling and the geometry of the shear lips were identical on the specimens tested at both rates. Scanning electron microscope fractography at 40X and 400X showed that the crack extension was completely ductile regardless of the test rate. A small initial stretch zone or crack tip blunting region was present on all specimens of approximately 30  $\mu$ m, after which the transition to ductile fracture (microvoid coalescence, dimpled rupture) was distinct. Scanning microscope fractographs are shown in Figure 14 of a dynamically loaded specimen compared to that of a similar static test. Both specimens were of the same HY-130 steel plate, with 20% side grooves, and an initial  $a/W$  of 0.65. Similar fracture processes are apparent in both specimens. Dimples of two distinct sizes were present on the fracture surface with the smaller 2- $\mu$ m size covering the large majority of the surface area. Large elongated dimples occurred occasionally in the range of 10 x 50  $\mu$ m oriented with the long axis in the direction of crack extension. The fracture surfaces resulting from both loading rates were typical of those found in static tests of ductile structural steels (i.e., without features which might suggest that the more rapidly loaded specimens demonstrated a significantly higher toughness).

## CONCLUSIONS

The major result of this work has been to demonstrate that  $J_I$ - $R$  curves and  $J_{Ic}$  values can be obtained from compact specimens of a structural steel loaded at rates five orders of magnitude higher than that used in static tests.  $J_I$ - $R$  curves were developed here for compact specimens of varying crack length loaded dynamically at load-line displacement rates of 9 *ips*. These  $J_I$ - $R$  curves were developed using a key curve methodology introduced by Ernst, et al,<sup>12</sup> and applied by Joyce to static tests of HY-130 steel<sup>13</sup> and A533B steel.<sup>18</sup>

The  $J_I$ - $R$  curves derived from the dynamically loaded tests were elevated with respect to the static results, with both  $J_{Ic}$  and tearing modulus values being increased. The accuracy of the dynamic  $J_I$ - $R$  curves obtained using the key curve method was verified in that the method accurately estimates the magnitude of final crack extension to 0.20 in. (5.08 mm). The fracture surfaces of the static and dynamically loaded HY-130 were similar in appearance. On the macroscopic scale, both showed similar shear lip development and crack

tunneling. For the temperature and loading rates used in this study, the fracture surfaces on a microscopic scale were completely ductile.

#### ACKNOWLEDGMENT

The authors are indebted to Mr. J. P. Gudas, Head of the Fatigue and Fracture Branch of this Center, for his support, guidance, and assistance in this research effort.

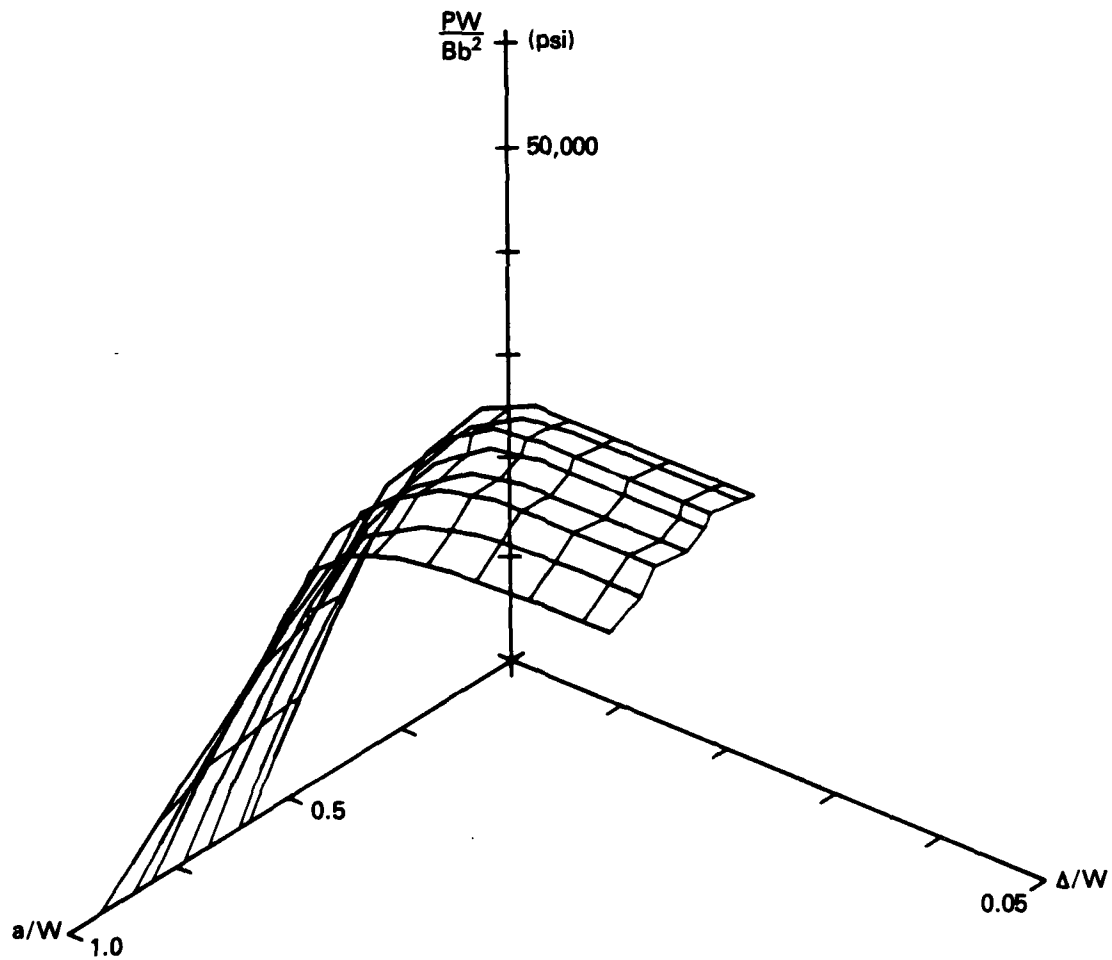


Figure 1 — Experimental Key Curve Function for HY-130 Steel for Static Loading Rate

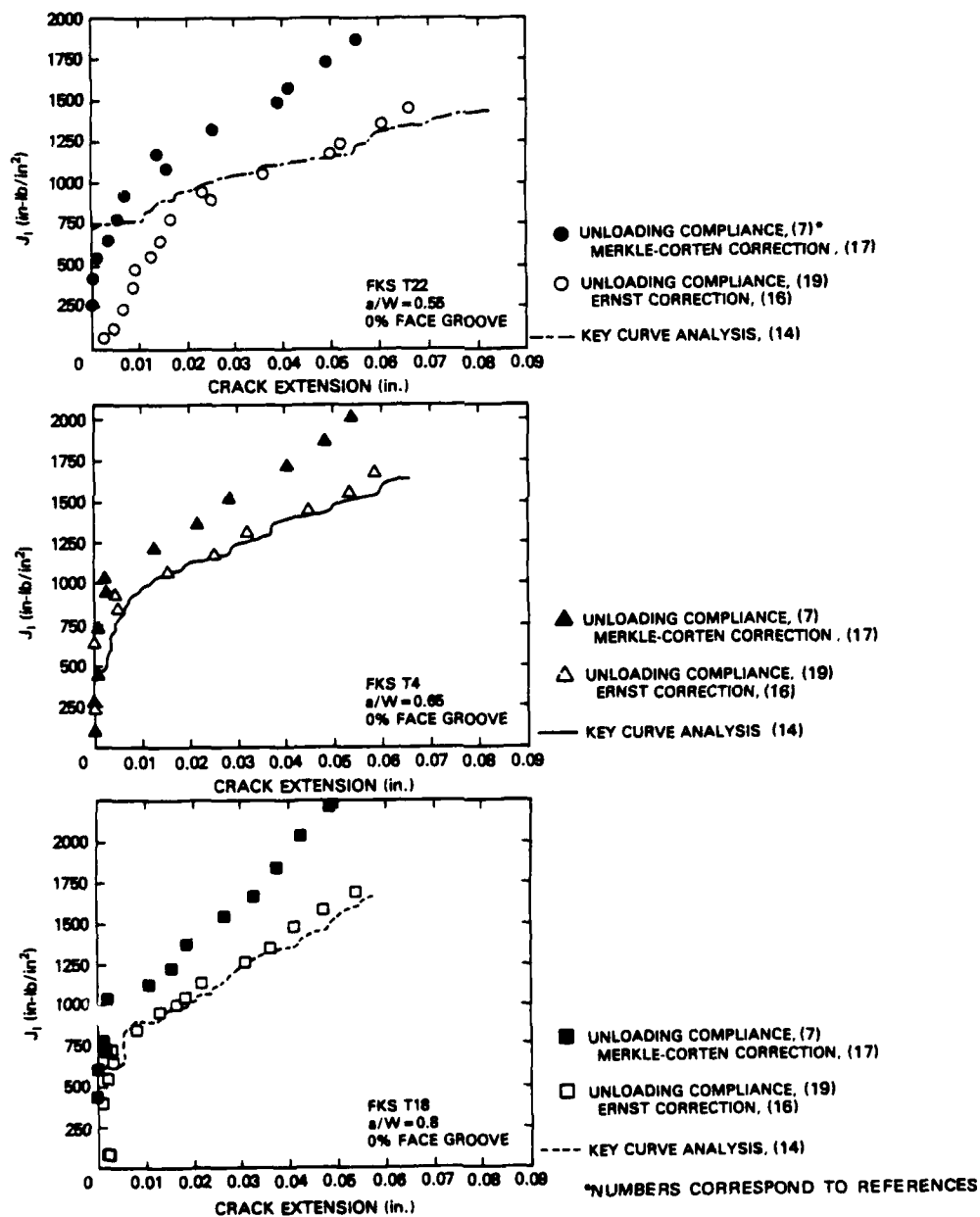
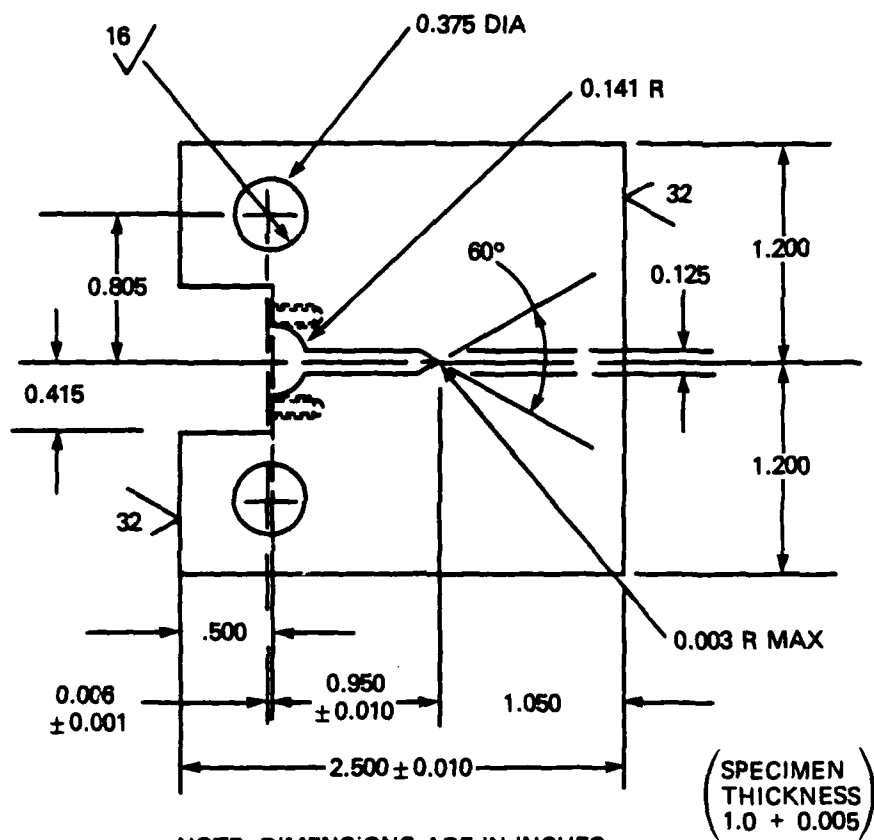
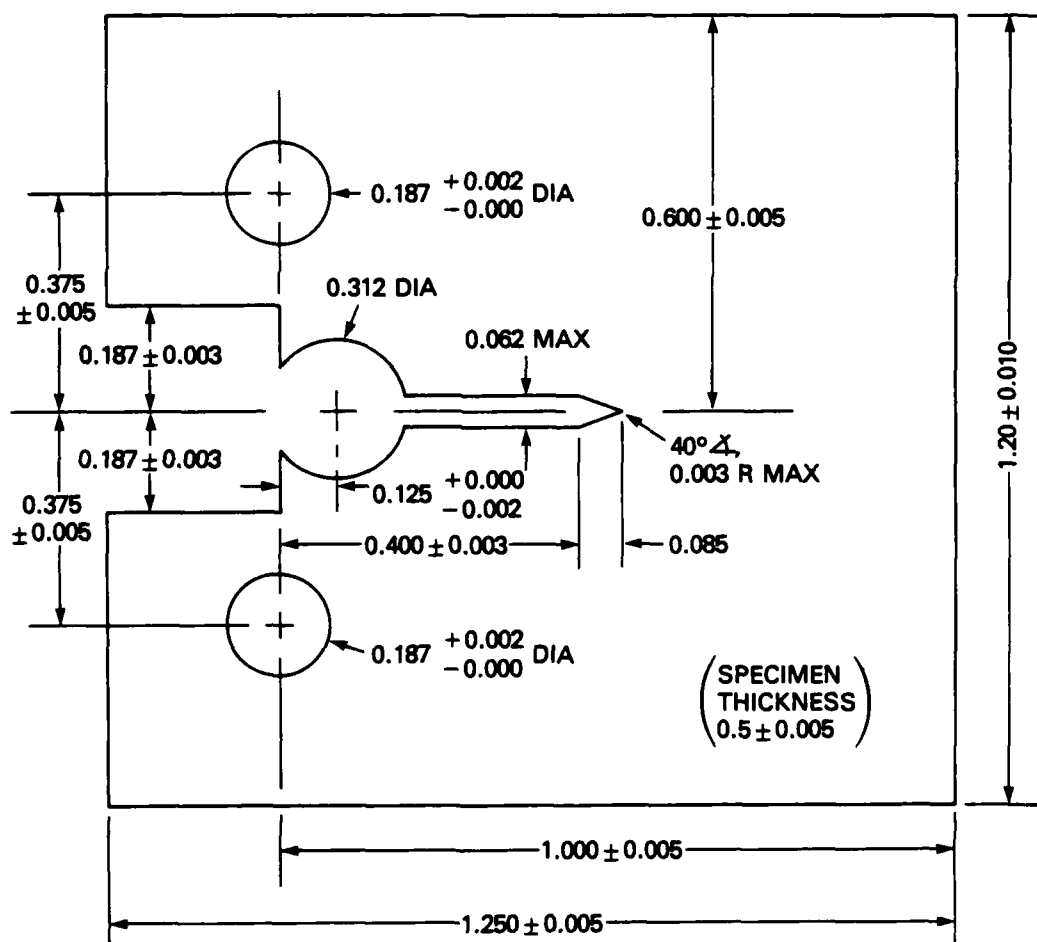


Figure 2 — HY-130  $J_I$ - $R$  Curves Developed by Key Curve Analysis and Unloading Compliance Under Static Loading Conditions



NOTE: DIMENSIONS ARE IN INCHES.

Figure 3 — Modified 1-Inch-Thick (25.4-mm) Compact Test Specimen for J-Integral Testing



NOTE: DIMENSIONS ARE IN INCHES.

Figure 4 — Modified 1/2-Inch-Thick (12.7-mm) Compact Test Specimen for J-Integral Testing

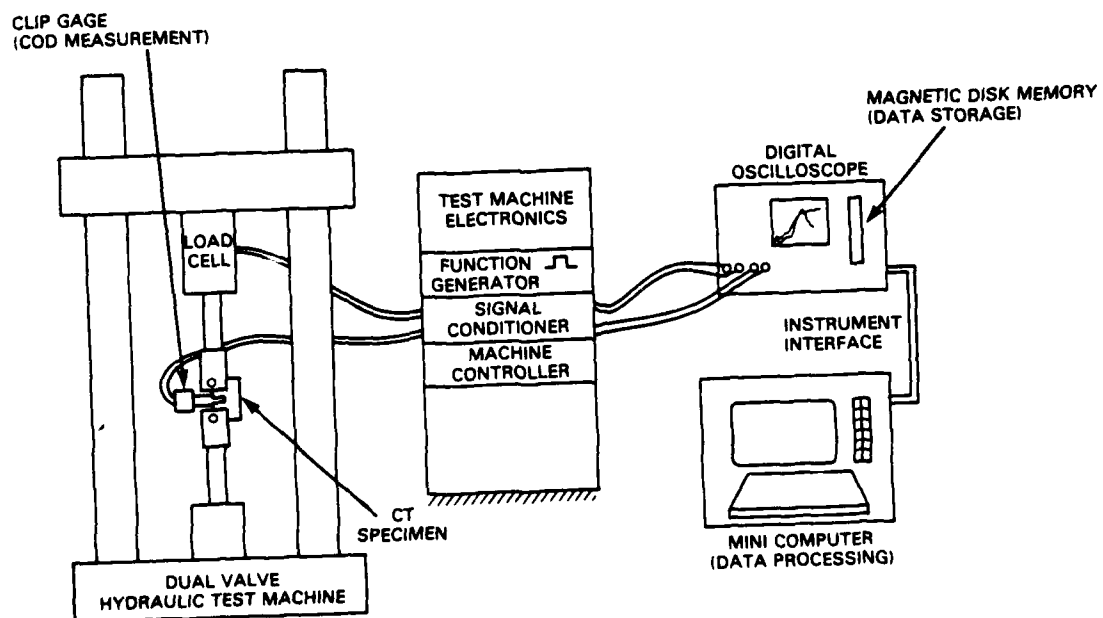


Figure 5 — Schematic of Compact Specimen Dynamic Test Arrangement

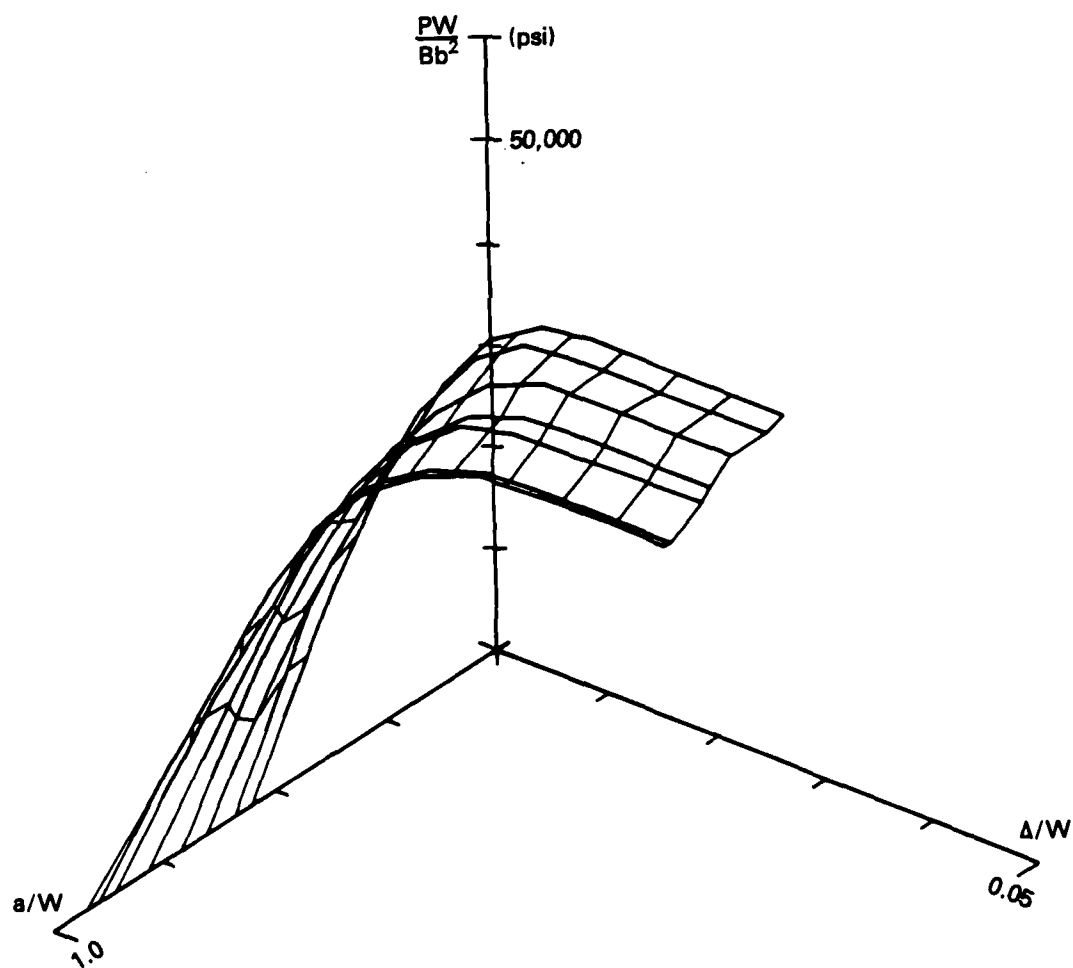


Figure 6 — Experimental Key Curve Function for HY-130 Steel Obtained Under Dynamic Loading

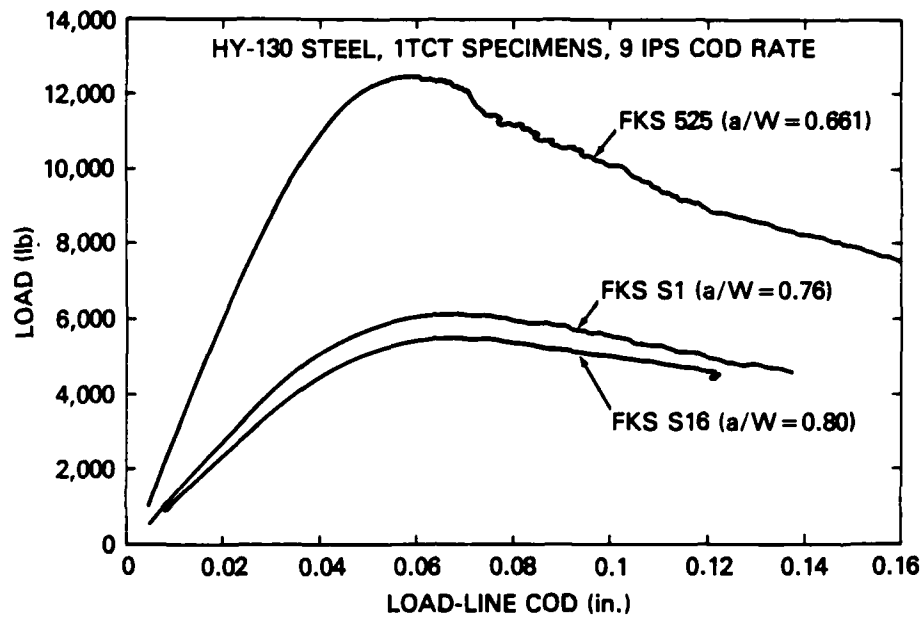


Figure 7 — Load-Displacement Curves for 1-Inch-Thick (25.4-mm) Compact Test Specimens of HY-130 Steel Tested Under Dynamic Loading Conditions

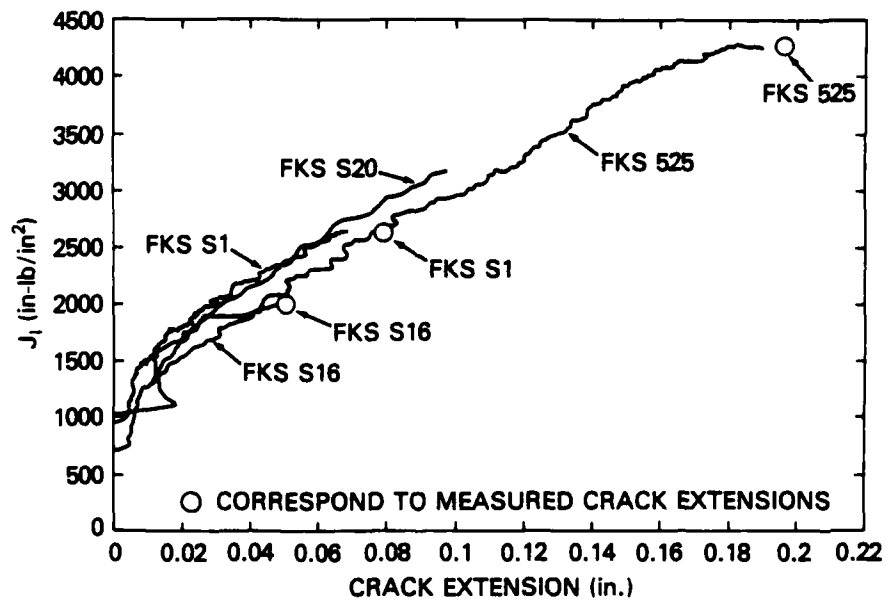


Figure 8 — J-Integral R-Curve for 1-Inch-Thick (25.4-mm) Compact Test Specimens of HY-130 Steel Tested Under Dynamic Loading Conditions

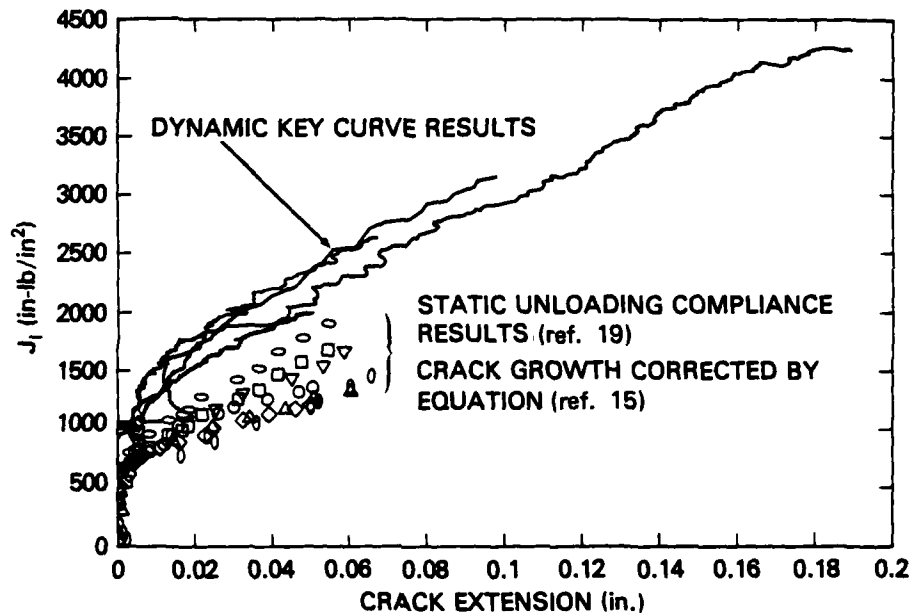


Figure 9 — J-Integral R-Curves for 1-Inch-Thick (25.4-mm) Compact Test Specimens of HY-130 Steel Tested Under Static and Dynamic Loading Conditions

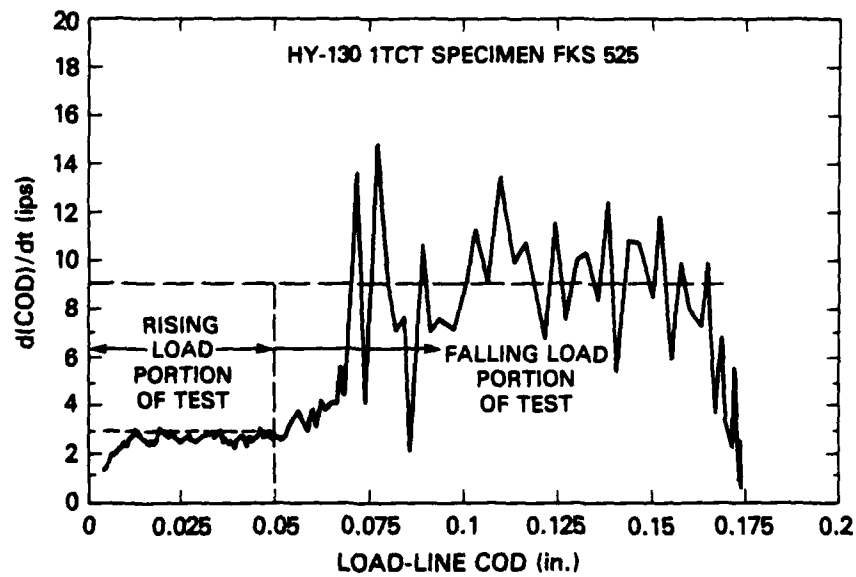


Figure 10 — Load-Line Crack-Opening Displacement Rate Versus Crack-Opening Displacement for a Typical 1-Inch-Thick (25.4-mm) Compact Test Specimen of HY-130 Steel Tested Under Dynamic Loading Conditions

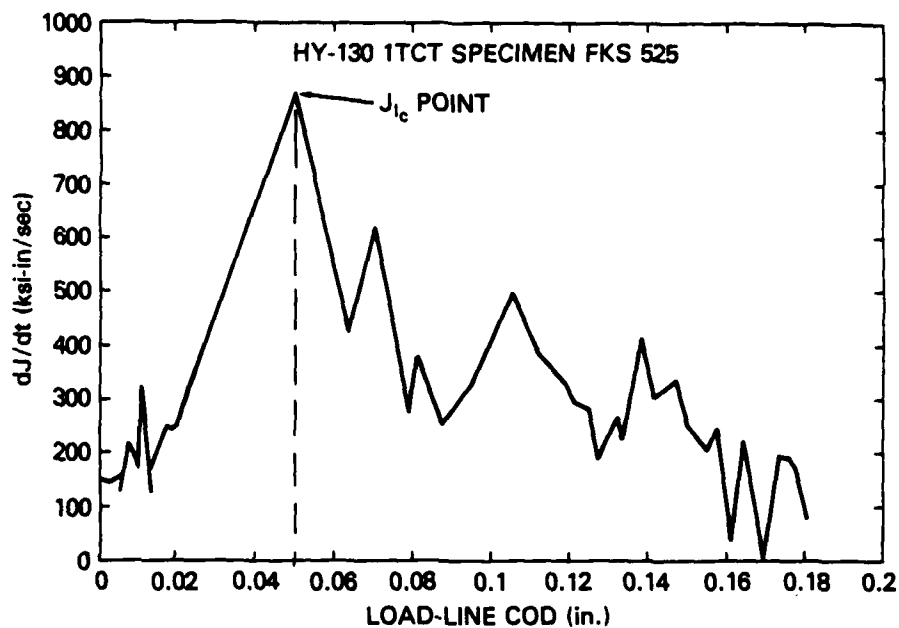


Figure 11 —  $dJ/dt$  Versus Crack-Opening Displacement for a Typical 1-Inch-Thick (25.4-mm) Compact Test Specimen of HY-130 Steel Tested Under Dynamic Loading Conditions

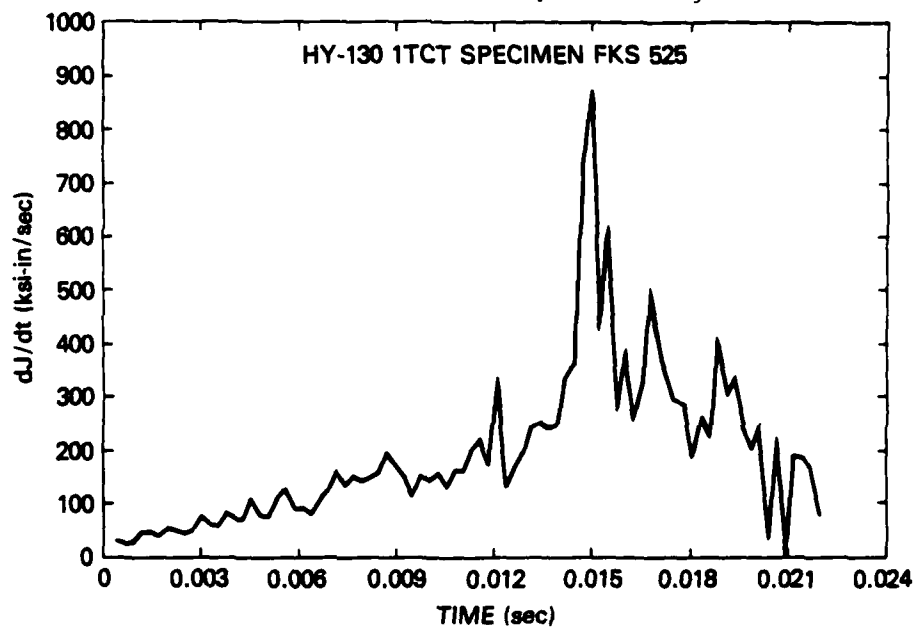


Figure 12 —  $dJ/dt$  Versus Elapsed Time for a Typical 1-inch-Thick (25.4-mm) Compact Test Specimen of HY-130 Steel Tested Under Dynamic Loading Conditions

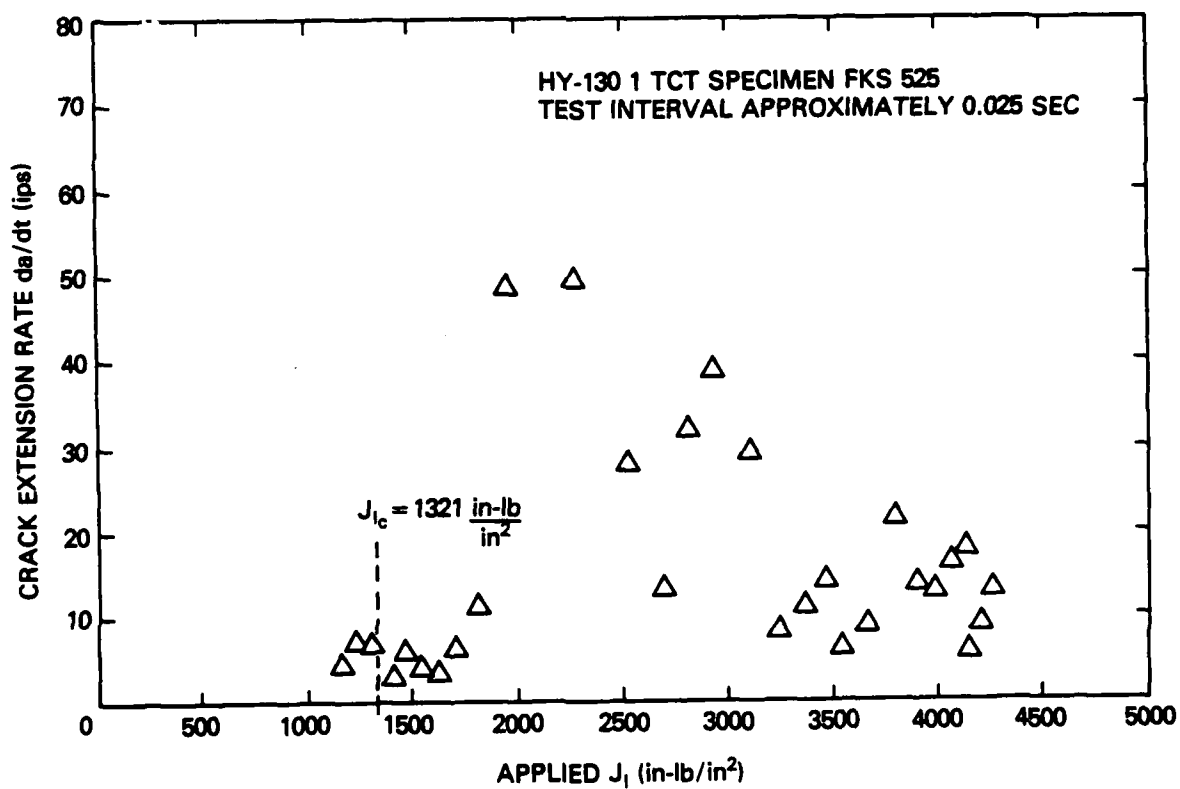


Figure 13 — Crack Extension Rate (Crack Velocity) Versus  $J_I$  for a Typical 1-Inch-Thick (25.4-mm) Compact Test Specimen of HY-130 Steel Under Dynamic Loading Conditions

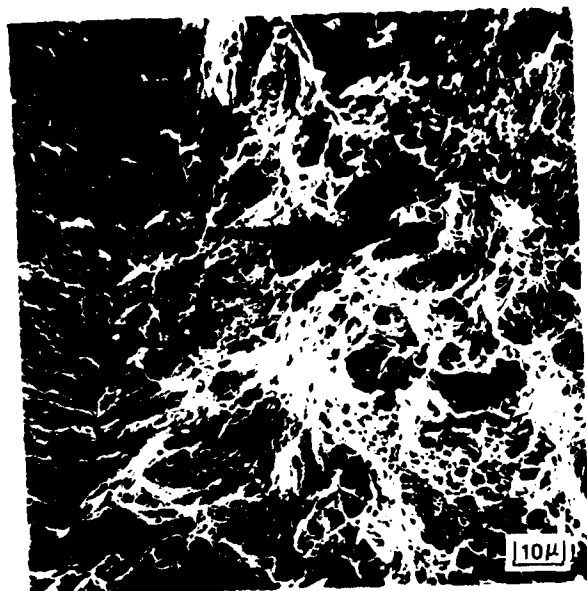


Figure 14a  
Static Loading

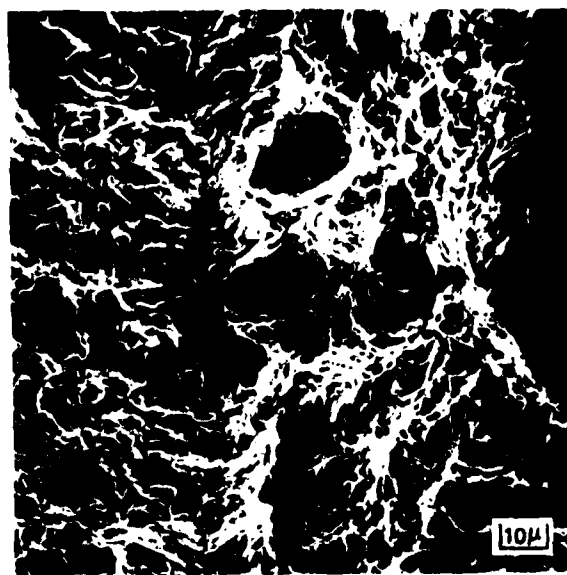


Figure 14b  
Dynamic Loading

Figure 14 Scanning Electron Fractographs of HY 130 Steel Ductile Fracture  
Crack Extension Under Static and Dynamic Loading (400X)

## REFERENCES

1. Rice, J.R., "A Path Independent Integral and the Approximate Analysis of Strain Concentrations by Notches and Cracks," *Journal of Applied Mechanics*, pp. 379-386 (Jun 1968).
2. Landes, J.D., and J.A. Begley, "Test Results from  $J$  Integral Studies: An attempt to Establish a  $J_{Ic}$  Testing Procedure," *Fracture Analysis*, ASTM STP 560, pp. 170-186 (1974).
3. Paris, P.C., "Fracture Mechanics in the Elastic-Plastic Regime," *Flaw Growth and Fracture*, ASTM STP 631, pp. 3-27 (1977).
4. Clarke, G.A., *et al*, "A Procedure for the Determination of Ductile Fracture Toughness Values Using the  $J$  Integral Technique," *Journal of Testing and Evaluation*, Vol. 7, No. 1 (Jan 1979).
5. Paris, P.C., *et al*, "Initial Experimental Investigation of Tearing Instability Theory," *Elastic-Plastic Fracture*, ASTM STP 668, pp. 251-265 (1979).
6. Joyce, J.A. and M.G. Vassilaros, "An Experimental Evaluation of Tearing Instability Using the Compact Specimen," presented at the 13th National Symposium on Fracture Mechanics, ASTM, Philadelphia, PA (June 1980).
7. Gudas, J.P., *et al*, "Investigation of Specimen Geometry Modifications to Determine the Conservative  $J_I$ - $R$  Tearing Modulus Using the HY-130 Steel System," *Fracture Mechanics*, ASTM STP 677, pp. 474-485 (1979).
8. Vassilaros, M.G., *et al*, "Effects of Specimen Geometry on the  $J_I$ - $R$  Curve for ASTM A533B Steel," *Fracture Mechanics*, ASTM STP 700, pp. 251-270 (1980).
9. Clarke, G.A., *et al*, "Single Specimen Tests for  $J_{Ic}$  Determination," *Mechanics of Crack Growth*, ASTM STP 560, pp. 27-42 (1976).
10. Hasson, D.F., and J.A. Joyce, "The Effect of a Higher Loading Rate on the  $J_{Ic}$  Fracture Toughness Transition Temperature of HY Steels," accepted for publication by *J. Engineering Materials and Technology*, ASME (1981).
11. Nguyen, P., *et al*, "The Determination of the  $J$ -Integral on Precrack Charpy Specimens by Instrumented Impact Testing and Slow Bend Testing" *Journal of Engineering Materials and Technology*, Vol. 100, pp. 253-257 (Jul 1978).
12. Server, W.L., "Static and Dynamic Fibrous Initiation Toughness Results for Nine Pressure Vessel Materials," *Elastic-Plastic Fracture*, ASTM STP 668, pp. 493-514 (1979).
13. Ernst, H., *et al*, "Analysis of Load-Displacement Relationships to Determine  $J$ - $R$  Curve and Tearing Instability Material Properties," *Fracture Mechanics*, ASTM STP 677, pp. 581-599 (1979).
14. Joyce, J.A., *et al*, "Direct Evaluation of  $J$ -Resistance Curves from Load-Displacement Records," *Fracture Mechanics*, ASTM STP 700, pp. 222-236 (1980).

15. Rice J.R., *et al*, "Some Further Results of J-Integral Analysis and Estimates," *Progress in Flaw Growth and Fracture Toughness Testing*, ASTM STP 536, pp. 231-245 (1973).
16. Ernst, H.A., *et al*, "Estimations on J-Integral and Tearing Modulus T from a Single Specimen Test Record," Westinghouse Scientific Paper 80-103-JINTF-P3, Pittsburgh, PA (May 1980).
17. Merkle, J.G., and H.T. Corten, "A J-Integral Analysis for the Compact Specimen, Considering Axial Force as Well as Bending Effect," *Journal of Pressure Vessel Technology*, pp. 286-292 (Nov 1974).
18. Joyce, J.A., "Application of the Key Curve Method to Determining  $J_I$ -R Curves for A533B Steel," NUREG/CR-1290 U.S. Nuclear Regulatory Commission, Washington, DC (Jan 1980).
19. Gudas, J.P., *et al*, "A Summary of Recent Investigations of Compact Specimen Geometry Effects on the  $J_I$ -R Curve of High Strength Steels," U.S. Nuclear Regulatory Commission Report NUREG/CR-1813 (Nov 1980).

# INITIAL DISTRIBUTION

## Copies

- 11 NAVSEA
  - 2 SEA 05D2
  - 1 SEA 05R15
  - 1 SEA 32B
  - 2 SEA 3233 (I. Fioritti)
  - 1 SEA 3233 (R. Provencher)
  - 1 SEA 3233 (D. Nichols)
  - 1 SEA 3233 (A. Spero)
  - 2 SEA 99612
- 12 DTIC
- 4 ONR
  - 2 Code 471
  - 2 Code 474
- 5 NRL
  - 1 Code 6300
  - 2 Code 6380
  - 2 Code 6384
- 19 U.S. Naval Academy, Annapolis, MD 21402
  - 1 Prof. T. Butler (Stop 11c)
  - 2 Dr. R. Mathieu (Stop 1)
  - 15 Prof. J. Joyce (Stop 11c)

## CENTER DISTRIBUTION

Copies	Code	Name
1	17	W. Murray
1	1702	J. Corrado
1	172	M. Krenzke
1	1720.1	T. Kiernan
1	1720.3	R. Jones, Jr.
3	1720.4	A. Wiggs
1	173	A. Stavovy
1	174	I. Hansen
1	177	
1	1770.1	V. Bloodgood
1	28	J. Belt
2	2803	V. Schaper
1	2809H	J. Hudak
5	281	G. Wacker
15	2814	J. Gudas
1	282	J. Crisci
1	522.1	Unclass Lib.
2	5231	Office Services

**DTNSRDC ISSUES THREE TYPES OF REPORTS**

1. DTNSRDC REPORTS, A FORMAL SERIES, CONTAIN INFORMATION OF PERMANENT TECHNICAL VALUE. THEY CARRY A CONSECUTIVE NUMERICAL IDENTIFICATION REGARDLESS OF THEIR CLASSIFICATION OR THE ORIGINATING DEPARTMENT.

2. DEPARTMENTAL REPORTS, A SEMIFORMAL SERIES, CONTAIN INFORMATION OF A PRELIMINARY, TEMPORARY, OR PROPRIETARY NATURE OR OF LIMITED INTEREST OR SIGNIFICANCE. THEY CARRY A DEPARTMENTAL ALPHANUMERICAL IDENTIFICATION.

3. TECHNICAL MEMORANDA, AN INFORMAL SERIES, CONTAIN TECHNICAL DOCUMENTATION OF LIMITED USE AND INTEREST. THEY ARE PRIMARILY WORKING PAPERS INTENDED FOR INTERNAL USE. THEY CARRY AN IDENTIFYING NUMBER WHICH INDICATES THEIR TYPE AND THE NUMERICAL CODE OF THE ORIGINATING DEPARTMENT. ANY DISTRIBUTION OUTSIDE DTNSRDC MUST BE APPROVED BY THE HEAD OF THE ORIGINATING DEPARTMENT ON A CASE-BY-CASE BASIS.

END

DATE  
FILMED

12-81

DTIC